International Journal of Heat and Mass Transfer 234 (2024) 126156

Contents lists available at ScienceDirect

International Journal of Heat and Mass Transfer

journal homepage: www.elsevier.com/locate/ijhmt

The effect of surface roughness on sessile droplet evaporation dynamics of silica nanofluid

Zhihao Zhang , Yuying Yan *

Faculty of Engineering, University of Nottingham, UK

ARTICLE INFO

Keywords:
Sessile droplet
Nanofluid
Surface roughness
Droplet evaporation

ABSTRACT

This study focuses on the influence of copper surface roughness on evaporation dynamics and deposition mode of fixed silica nanofluid droplets. It aims to achieve an enhanced cooling effect based on silica nanofluid spray. The results show that roughness significantly impacts copper surface wettability. As roughness decreases, the evaporation lifetime of silica nanofluid droplets would be prolonged, by up to 75 %. Increasing the roughness will also increase the temperature of the droplet apex, and the temperature difference between the top of the droplet; the contact line area will also be reduced by up to 54 %, inhibiting the evaporative cooling effect. Roughness also significantly impacts the deposition pattern of nanofluid droplets. The coffee ring effect is produced on all kinds of surfaces. Still, the coffee ring effect is suppressed as the roughness increases, and the coffee ring deposition has a very small number of fractures on smooth surfaces with more minor roughness. In contrast, on rough surfaces, the number of fractures increases significantly. In summary, this experimental study reveals the critical influence of the roughness of copper, a widely used heat dissipation material, on the heat and mass transfer process and sedimentary pattern of silica nanofluid droplet evaporation.

1. Introduction

Droplet evaporation is one of the most common physical processes in nature. Since Maxwell first deduced the equations of droplet evaporation based on the diffusion process in the still air in 1877 [1], experimental and numerical studies on droplet wetting and evaporation have become increasingly and more in-depth. Nowadays, the physical phenomenon of droplet evaporation is used widely, such as spray cooling [2], ferrofluid heating [3], inkjet printing [4], surface coating [5], biopharmaceutical [6], combustion engine fuel [7], and semiconductor device manufacturing [8]. Among them, due to the efficient energy transport characteristics of nanofluids, the evaporation of nanofluid droplets has received widespread attention and has been widely used in various fields [9-12]. Due to the contained nanoparticles, it not merely affects the evaporation dynamics but also leads to depositional processes on the surface, such as the classic coffee-ring effect [13], which was first proposed in 1997 by Deegan et al. [14]. Therefore, it is natural to associate that in addition to nanofluidic properties, the characteristics of the surfaces contacted by the droplets will strongly influence their evaporation and deposition processes. Hence, as one of the primary surface properties, surface roughness has been widely considered in engineering and scientific research [15], such as surface coating [16], cooling efficiency [17], and even contact killing of bacteria [18]. Moreover, surface roughness could also significantly impact the droplet heat and mass transfer process during evaporation [19], owing to its effect on surface morphology, surface free energy, wettability, and heat transfer efficiency. Based on this, it can be judged that surface roughness will significantly impact the heat dissipation effect of thermal management methods based on droplet evaporation, such as spray cooling. Therefore, it is crucial to reveal the impact of surface roughness on the nanofluid droplet evaporation dynamics and sedimentary pattern.

The roughness degree is a critical issue in the evaporation process. Surface roughness could influence the wetting phenomenon [20]. Besides, the surface roughness could also impact the sessile droplet evaporation dynamics like contact line moving [21], evaporation mode [22], and evaporation rate [19]. Therefore, the total evaporation time and average evaporation rate of the sessile droplet also changed accordingly owing to these effects. Kumar et al. [23] pointed out that the characteristic of surface roughness is sufficient to cause the contact line pinning phenomenon during droplet evaporation, thus having a significant impact on droplet evaporation dynamics. Nguyen et al. [24] indicated that with the increase of surface hydrophobicity, the evaporation time

* Corresponding author.
E-mail address: yuying.yan@nottingham.ac.uk (Y. Yan).

https://doi.org/10.1016/j.ijheatmasstransfer.2024.126156
Received 3 April 2024; Received in revised form 8 August 2024; Accepted 31 August 2024
Available online 4 September 2024

can also be prolonged, and lots of similar studies have also verified this phenomenon [19]. Zhang et al. [25] fabricated four surfaces with different roughness on a steel substrate and found that they were all hydrophilic, and the contact angle of the water droplets decreased with increasing roughness. Bussonnière et al. [26] also pointed out that the Cassie–Baxter state of the droplet could be prolonged with the increase of roughness on the hydrophobic micro/nano-structures surface. Chen et al. [27] revealed that the critical transition of the Cassie-Baxter state to the Wenzel state has a strong relationship with the surface roughness for the sessile droplet, and based on this, they pointed out that the surface with hierarchical roughness would effectively suppress this critical transition and constant contact radius (CCR) mode. Huang et al. [28] designed a model with different roughness based on silicon substrates. The research results show that when the roughness decreases, the proportion of the total time of the droplet constant contact angle (CCA) mode also increases. Gunjan et al. [29] proposed to integrate the dynamic roughness changes caused by air pollutants into the classical evaporation model, and the new model can predict the process of droplet evaporation on the surface of the silicon pillar and the change of the evaporation mode. Siddiqui et al. [30,31] found that a porous structure with different pore sizes and areal porosity would form on the surface after the nanofluid droplet evaporation, and the surface roughness of residue will also increase with porosity, which will increase the evaporation rate of subsequent droplets. However, studies about the influence of surface roughness on the sessile nanofluid droplet evaporation process are still rare, and the mechanism of the effect of surface roughness on the evaporation heat transfer of nanofluid droplets is still unclear. Therefore, the effects of surface roughness on the sessile silica nanofluids droplet evaporation remain elusive and need to be explored in depth.

As mentioned above, the surface roughness could significantly influence the sessile droplet wetting and evaporation process. Naturally, it also plays a vital role in the sedimentary pattern of particle-laden droplets [32,33]. Batishcheva et al. [32] found that the ring sedimentary pattern was formed on the aluminium-magnesium alloy surface when the droplet loaded 0.025 % v/v polystyrene (PS) particles, and when the concentration increased to 0.3 % v/v, a spot-like sedimentary pattern was formed which owing to the presence of multimodal roughness on the surface treated with laser radiation. Mulka et al. [34] also explore the drying process of silica nanofluid droplets on copper and stainless-steel substrates with different degrees of surface roughness. They found two types of crack formation: logarithmic spiral and straight radially oriented. The spiral cracks are due to deposition delamination, while the interaction of capillary pressure and shear stress between the coating and the substrate causes straight cracks. Liu et al. [35] also found that when silica nanofluid droplets were evaporated on glass substrates with different roughness, the crack spacing produced by the sedimentary pattern became smaller with increasing roughness. Wąsik et al. [36] also studied the Bénard−Marangoni (BM) cell sedimentary pattern effect produced when ZnO nanofluid droplets evaporate on different substrates, and the results showed that the BM deposition patterns produced on glass surfaces with minimal roughness have the most minor diameters and density. Kubochkin et al. [37] performed droplet sedimentary pattern studies with CdTe nanofluids and found that button-like patterns were formed on polypropylene-sprayed surfaces with significant maximum roughness while coffee-ring sedimentary patterns were produced on other smooth surfaces. Meanwhile, Kim et al. [38] pointed out that the difference in the surface roughness of each sample is reduced due to the deposition of nanoparticles on the surface during the evaporation, which makes the effect of roughness on the evaporation heat transfer of nanofluid droplets insignificant. Liu et al. [39] also pointed out that the surface roughness of the substrate is an essential factor in affecting the sedimentation of particles loaded by nanofluidic droplets. They found that the internal flow would be inhibited, and the Marangoni effect would also be weakened with the increase of surface roughness, making the sedimentation distribution even and slow. Charitatos et al. [33] also pointed out that surface roughness strongly affects the sedimentary pattern of nanoparticle-laden droplets on the inclined substrates. Moreover, as far as the authors' knowledge, not many reports in the literature have clarified a description of the relationship between the surface roughness and the nanofluid droplet sedimentary pattern until now.

In the wide range of applications of droplet evaporation, silica nanofluids are increasingly involved, and the sedimentary characteristics of droplets loaded with nanoparticles also significantly affect the effects of various industrial applications and products. At the same time, copper is a commonly used industrial metal material, so studying the effect of copper surface roughness on the heat and mass transfer mechanism during the evaporation of silica nanofluid droplets is significant. Therefore, this study mainly reveals the heat and mass transfer mechanisms at the liquid-vapour interface of silica nanofluid droplets and explores the effect of surface roughness on the solid-liquid interface on the sedimentary pattern of nanofluid droplets. Ultimately, based on the experimental results and theoretical analysis, this study shows that surface roughness significantly affects the wettability of copper surfaces and the evaporation dynamics of silica nanofluid droplets. The findings also indicate that the substrate surface roughness significantly affects the coffee-ring effect of the nanoparticle sedimentary pattern. This study helps reveal the interaction mechanism between surface roughness, nanofluid droplet evaporation dynamics, and sedimentary process, which is expected to guide related industrial applications and scientific analysis.

2. Experimental setups and methodology

Before the experiment, the environmental conditions of the closed laboratory were measured, and the relative humidity in the laboratory was about 50 ± 5 %, which was detected automatically; the ambient temperature and air pressure were 293 ± 2 K and 0.1 MPa, respectively. Under these well-controlled conditions, the experimental measurements are highly reproducible. The experimental processes are shown in Fig. 1. As shown in Fig. 1, the contact angle and droplet shape change measured by the Optical Profilometer (Biolin Scientific, Finland), and the liquid-vapor interface temperature distribution of the sessile nanofluid droplet was also observed by the Infrared Camera (FLIR LLC, USA).

The fluids used in the experiments are deionized (DI) water and silica nanofluid, in which silica nanoparticles (SNP) were dispersed in DI water (RS PRO, UK) and followed by ultrasonication for two hours based on the two-step method. The silica nanoparticles (Sigma-Aldrich, USA) with a diameter of 0.007 μm were used in this study and were prepared at a fixed particle concentration of 0.5 % volume fraction, respectively. A pipette (Eppendorf Corporate, Germany) generates the nanofluid droplet, which ensures a constant volume by pushing the working fluid out smoothly. Meanwhile, 2, 4, 6, and 8 μL are the droplet volumes used during the experiment.

2.1. Substrate surface preparation

As shown in Fig. 1, the copper discs were polished with emery paper (3 M Science, USA) through a lapping machine. The grid size of the emery papers is P120, P240, P400, and P1200, respectively. The optical microscope (OPTIKA Microscopes, Italy) with cold LED light observed the surface image and the deposition appearance. Besides, in this study, the surface roughness parameters of the substrate listed in Table 1 and the 3D colour view images shown in Fig. 1 were measured by the 3D optical profilometer (KLA Corporation, USA). The surfaces S1 to S4 are fabricated by P120, P240, P400, and P1200 emery paper through a grinding machine. The surface roughness parameters include S_a which means the roughness average, S_q means the root mean square roughness, S_p means the highest peak height, S_v means the absolute value of maximum pit height, and S_{sk} means the surface skewness. The

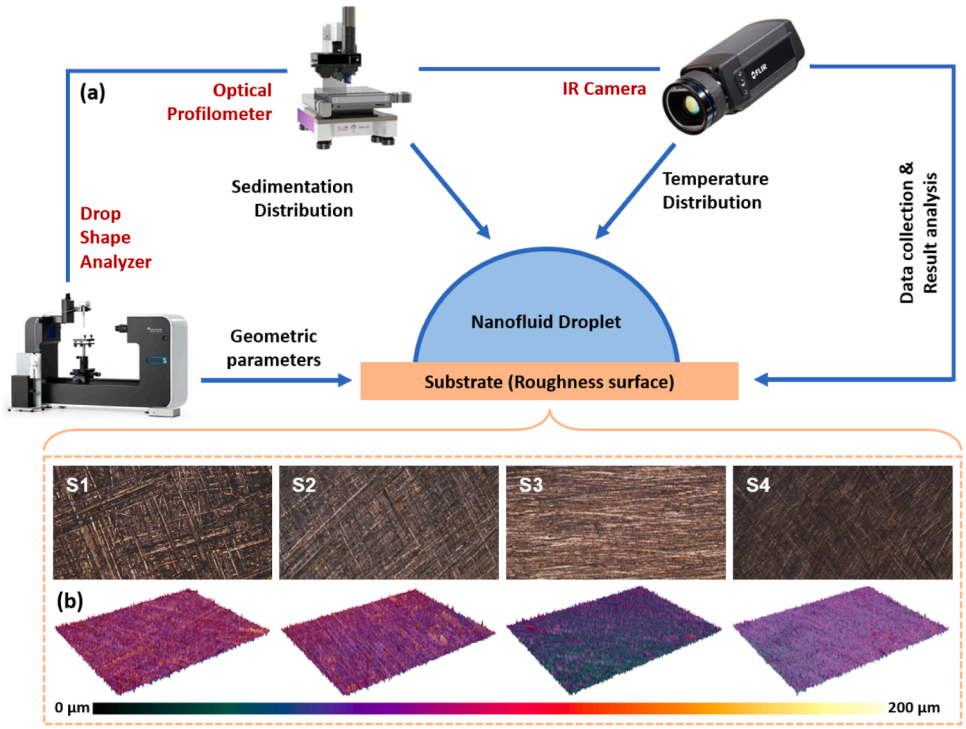

Fig. 1. (a) Schematic diagram of experimental device and process; (b) optical profiling of the sample surface.

Table 1
Surface roughness measurement data of copper disc samples.

Samples No.	S_a (μm)	S_q (μm)	S_p (μm)	S_v (μm)	S_{sk} (μm)
S1	15.86	20.64	96.19	84.25	−0.0343
S2	14.88	19.78	90.73	112.32	−0.6768
S3	13.97	18.83	99.02	110.05	−0.6919
S4	9.389	12.05	80.97	51.61	0.2265

calculation formula is shown in Eqs. (1-5). The copper discs are fixed on the water bath heater with silicone grease (RS PRO, UK), and the surface temperature is controlled at about 40 ± 2 ℃.

$$S_a = \frac{1}{A}\int_A \int |z(x,y)|dxdy \tag{1}$$

$$S_q = \sqrt{\frac{1}{A}\int_A \int (z(x,y))^2 dxdy} \tag{2}$$

$$S_p = \max_A z(x,y) \tag{3}$$

$$S_v = \left|\min_A z(x,y)\right| \tag{4}$$

$$S_{sk} = \frac{1}{S_q^3}\left[\frac{1}{A}\int_A \int z^3(x,y)dxdy\right] \tag{5}$$

It is essential to determine if the sessile droplet on the rough copper surfaces is a spherical cap to analyse the subsequent changes in the droplet shape. The effect of gravity on the droplet could be confirmed by the Bond number (*Bo*), a dimensionless number defined as the ratio of gravitational force to surface tension force. And usually, when the *Bo* is <1.0, the effect of the influence of gravity can be ignored, and surface tension dominates. The maximum value of the *Bo* number in this study is about 0.85, so all experimental groups can be regarded as meeting the requirements. The *Bo* can be calculated by using Eq. (6),

$$Bo = \frac{\Delta\rho r^2 g}{\sigma_{lg}} \tag{6}$$

where $\Delta\rho$ is the density difference between the liquid and air, r is the radius of the contact line, g is the gravitational acceleration, and σ_{lg} is the surface tension of the liquid. At the same time, the adhesion work is defined based on the Dupré equation [40] could be described as:

$$W_{AB} = Y_A + Y_B - Y_{AB} \tag{7}$$

where A and B mean phase or object, when the two objects are solid and liquid, respectively, the work of adhesion can also be described as:

$$W_{SL} = \sigma_S + \sigma_L - \sigma_{SL} \tag{8}$$

where σ_S means surface free energy, σ_L means surface tension of liquid, and σ_{SL} means interfacial tension between solid and liquid phase. Then, the simplified work of adhesion per unit area could be described as:

$$W_{PSL} = W_{SL}/A \tag{9}$$

where A is defined as the two-dimensional contact area of the liquid-vapour interface.

2.2. Silica nanofluid preparation

In this experimental study, the one-step method was used to prepare nanofluids, a standard method for preparing nanofluids [41-43]. The one-step method usually has the advantages of good dispersion and high suspension stability. In this article, the silica nanoparticles were directly dispersed into the base liquid deionized water, and then an ultrasonic generator was used for ultrasonic vibration and stirring for 2 h. In this experiment, the mass percentage concentration of silica nanofluid was 0.5 wt%. Besides, it needs to be mentioned that based on previous studies on the surface tension of silica nanofluids [44,45], the surface tension of 0.5 wt% nanofluid at 40 °C was estimated to be 63 mN/m.

3. Results and discussion

3.1. The effect of surface roughness on the droplet wettability

The surface wettability could be influenced significantly by the surface roughness. As seen in Fig. 2(a-d), the surface wettability also improved with the increase of the surface roughness degree. As shown in Fig. 2(a), for the 2 μL silica nanofluid droplet, when it is located on the S1 surface, the contact angle (CA) appears as 43° approximately. When the surface changes to the S2, S3, and S4, the apparent contact angle also increases to about 60°, 77°, and 92°, respectively. This is attributed to the inverse relationship between contact angle and roughness under hydrophilic surfaces. It also could be described as $cos\theta^* = r \cdot cos\theta$, which is also known as the Wenzel equation [46], where θ^* is the apparent contact angle, θ refers to Young's contact angle, r refers to surface roughness degree. As shown in Fig. 2(b-d), this phenomenon still occurs when the volume of silica nanofluid droplets increases. Although the initial apparent contact angle changes somewhat with the volume change, the overall difference is insignificant. It can be concluded that the impact of droplet volume on wettability is very limited. In addition, it is worth mentioning that on surfaces with different roughness, the difference in the contact angle hysteresis of the droplet is not apparent, which shows that the surfaces are generally hydrophilic. Then, as shown in Fig. 2(a-d), the surface roughness degree also significantly affects the silica nanofluid droplet evaporation lifetime. It is worth noting that the contact angle is too small in the final evaporation stage, making it difficult to measure directly. Therefore, for the convenience of analysis, the endpoint of the evaporation time of the curve in Fig. 2 is taken as an integer multiple of 50 s, and the final stage of evaporation is described by a dotted line fitting. As shown in Fig. 2(a), as the substrate surface changes from S1 to S4, the evaporation lifetime also extends from about 250 s to 400 s, increasing by about 60 %. As shown in Fig. 2 (b-d), as the surface roughness degree decreases, the evaporation lifetime of the sessile droplet also maximum prolongs about 66.7 %, 71.4 %, and 75 %, respectively. It can be concluded that on a hydrophilic surface, the increase in roughness will reduce the life of the silica nanofluid droplet, which may owe to the increase in roughness increases the contact area of the solid-liquid interface, enhances the heat transfer process, and promotes evaporation. Besides, the wettability can significantly affect the evaporation mode of droplets [47]. Similarly, in this study the surface roughness could also significantly affect the silica nanofluid evaporation mode. As shown in the dotted line in Fig. 2(a-d), regardless of the droplet volume, the evaporation mode of the droplets on the S1, S2, and S3 surfaces always remains in the constant contact radius (CCR) mode [48], which means that the droplet contact line (CL) is pinned. The contact angle continues to decrease during the evaporation process. However, on the S4 surface, during the last 10 %−20 % stage of evaporation of the droplet, the evaporation mode of the droplet will change from CCR to mixed mode [49], which refers to the process that the contact line and contact angle of the droplet move simultaneously. It may be because smoother surfaces have more minor energy barriers, lowering the energy and tension requirements needed to move the droplet contact line. Thus, as evaporation proceeds, the surface tension at the liquid-vapour interface drives the contraction of the contact line, which in turn gives rise to the slip phenomenon.

At the same time, the quantitative trend of droplet height H changes

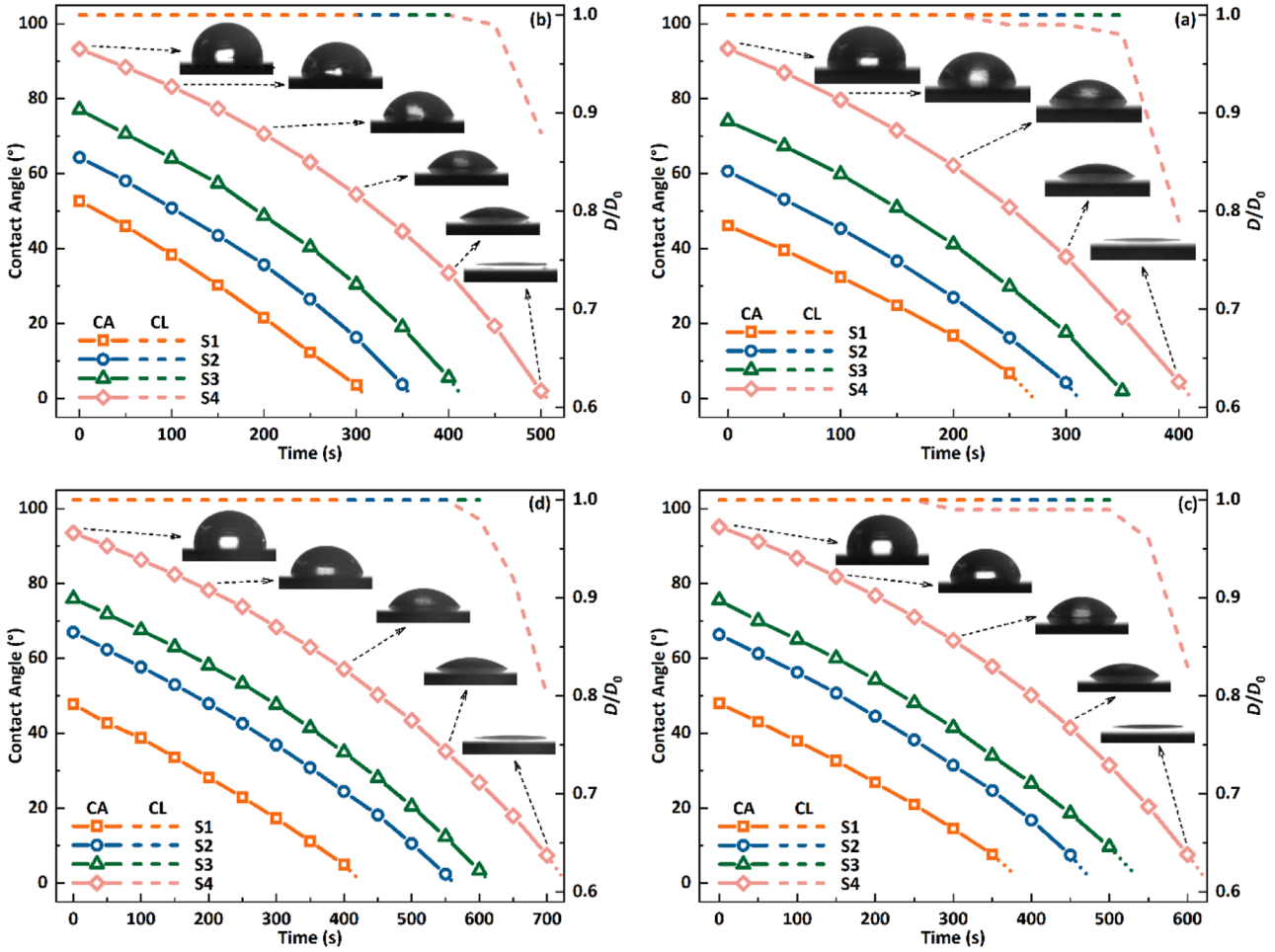

Fig. 2. Evolution of the contact angle of a sessile droplet with a volume of (a) 2, (b) 4, (c) 6, (d) 8 μL when located on substrates with different roughness.

is shown in Fig. 3(a-d). The degree of surface roughness has a significant effect on profile-changing trends. As shown in Fig. 3(a), with the increase of the surface roughness degree, the height of the silica nanofluid also keeps decreasing. Then, the inverse ratio of dimensionless height change with time is also shown in Fig. 3(a). Regardless of the surface roughness, the rate of change of the reciprocal of the dimensionless height of the droplet (H_0/H) increases significantly as the evaporation process proceeds, and they all rise sharply about fifty seconds before the evaporation process ends. As shown in Fig. 3(b-d), this trend also has the same appearance at the droplet volume of 4–8 μL. This may be because, during the evaporation process, the height of the droplets decreases. In the final evaporation stage, the evaporative cooling effect is weakened. This makes the relative evaporation rate of the droplets more significant, which in turn accelerates the droplet height shrinking velocity.

To further study the effect of copper surfaces with different roughness on the wettability of silica nanofluid droplets, based on the experimental results, the change of the work of adhesion (WoA) at the liquid-solid interface of the droplet during the evaporation process was calculated according to Eqs. (7-9), as shown in Fig. 4(a-d). As the surface roughness decreases, the work of adhesion between the droplet solid-liquid interface also decreases. Based on the individual volumes, the initial work of adhesion of the silica nanofluid droplet decreases by an average of about 45 % when the surface goes from S1 to S4. During the evaporation of the droplet, the magnitude of the adsorption work at the liquid-solid interface of the droplet on the surface with minor roughness is always lower. As time goes by, the work of adhesion of the liquid-solid interface gradually increases and eventually reaches a maximum value of about 137 mJ/m^2. These calculations show that the greater the roughness, the more work is required to separate the droplet from the surface and the stronger the wetting ability.

3.2. *The effect of surface roughness on the droplet interfacial heat transfer*

The effect of surface roughness on wettability was introduced in the previous section. This section will also introduce the influence of the surface roughness on the silica nanofluid droplet heat and mass transfer. Under different surface roughness, the temperature change trend at the top of the 2 μL silica nanofluid droplet with time is shown in the line chart in Fig. 5(a). It can be seen from Fig. 5(a) that with the increase of the surface roughness degree, the temperature at the top of the droplet (T_{top}) keeps increasing. The T_{top} increased from about 34.4℃ to 37.4 ℃, improving 8.7 %, when the substrate surface changed from S4 to S1. This may be because as the surface roughness degree increases, the droplet height becomes lower, which enhances the heat conduction process inside the droplet, thereby increasing the temperature of the liquid-vapour interface. Under other droplet volume conditions, the maximum increase in T_{top} is also around 8.7 %, meaning that volume changes have little impact. On the other hand, it can also be seen from the bar chart in Fig. 5(a) that as the roughness decreases, the maximum difference between the temperature at the top of the droplet and the temperature in the contact line area ($T_{diff,max}$) also becomes more significant. The $T_{diff,\ max}$ of the silica nanofluid droplet increased from about 1.3℃ on the surface S1 to about 2℃ on the surface S4, which is an increase of approximately 54 %. As the roughness increases, the evaporative cooling effect of the liquid-vapour interface is also enhanced, which may be due to the reduced surface wettability, inhibiting the heat

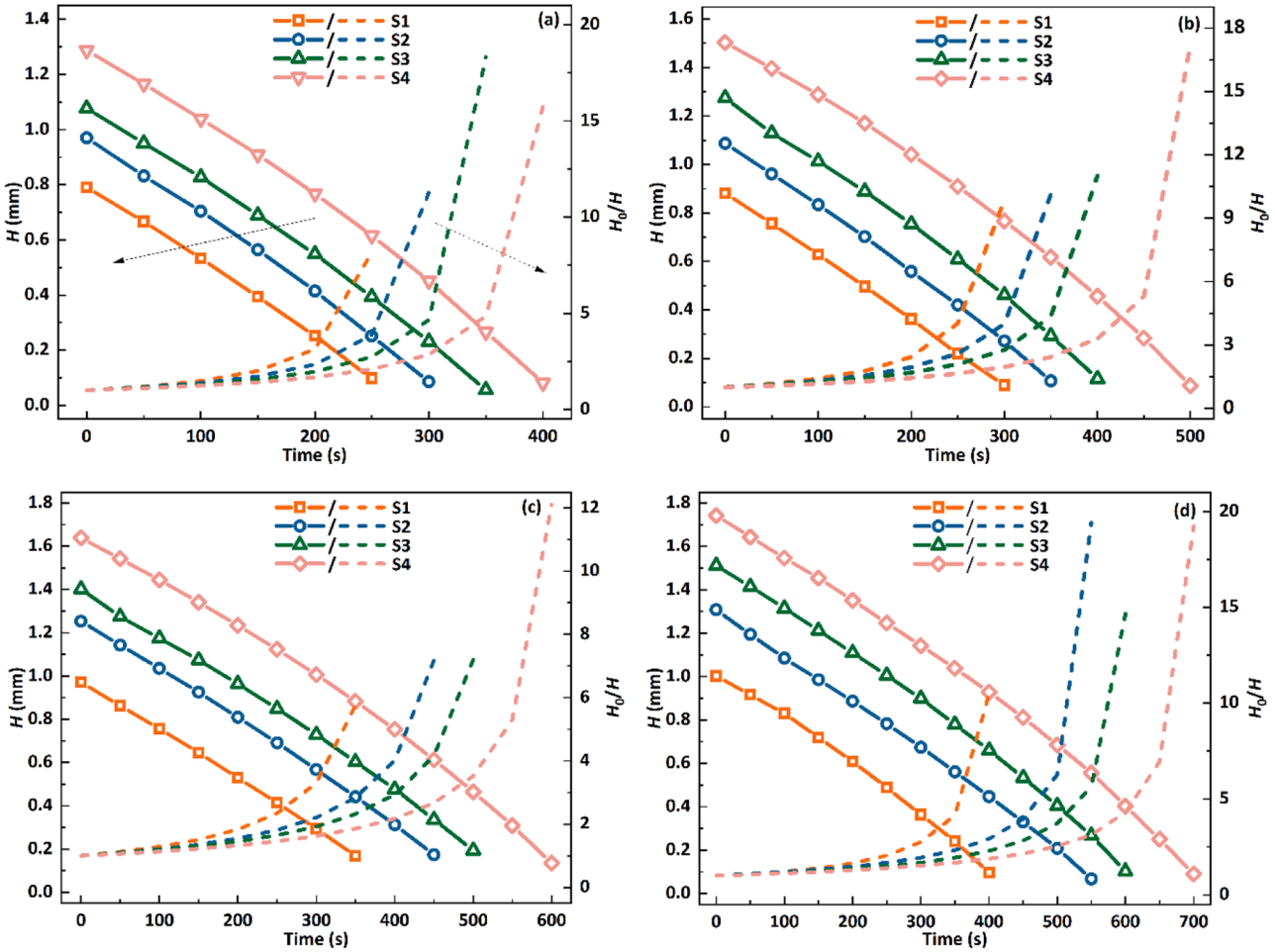

Fig. 3. The height shrinkage process of the (a) 2 μL, (b) 4 μL, (c) 6 μL, and (d) 8 μL droplets.

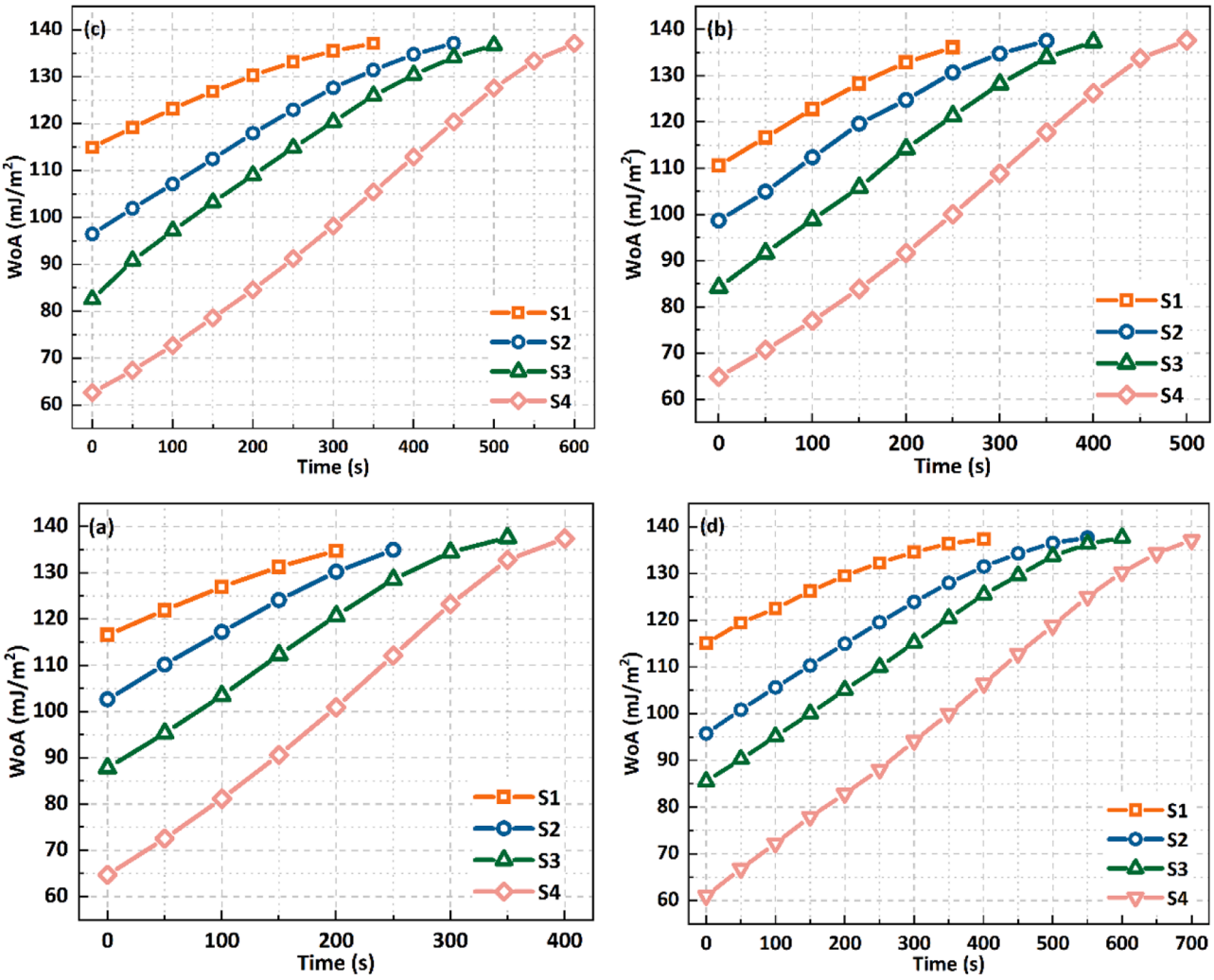

Fig. 4. Variation of adhesion work at the liquid-solid interface of a (a) 2 μL; (a) 4 μL; (a) 6 μL; (a) 8 μL droplet during evaporation.

transfer process inside the droplet, thus promoting the evaporative cooling effect. The $T_{diff,max}$ difference on the surface of S1 and S4 also change to 40 %, 35 %, and 32 % as the volume increases to 4 μL, 6 μL, and 8 μL, respectively. Then, these kinds of trends also remain unchanged, with the droplet volume gradually increasing to 4 μL, 6 μL, and 8 μL. As shown in Fig. 5 (b-d), the temperature at the droplet's top gradually increases and stabilizes at about 40℃. With the silica droplet volume increase, the T_{top} also decreases in the initial stage, like the S1 surface decline of about 2 %. It may be due to the droplet height increasing with droplet volume, suppressing droplets inside heat transfer and further enhancing the evaporative cooling effect, making the temperature of the liquid-vapour interface decline. At the same time, with the increase of silica nanofluid droplet volume, $T_{diff,max}$ also increases significantly, such as increasing by 25 % on the S4 surface from 2 μL to 8 μL, which could be attributed to the enhanced evaporative cooling effect.

Then, as shown in Fig. 6, the temperature distribution of the liquid-vapour interface of the silica nanofluid droplets of different volumes on the S4 surface. It can be seen from Fig. 6(a-d) that on the S4 surface, droplets with various volumes have a relatively pronounced evaporative cooling effect in the initial stage. At the liquid-vapour interface, the temperature in the top centre region is significantly lower than in the contact line region. As the evaporation proceeds, the temperature distribution at the liquid-vapour interface gradually becomes uniform, stabilizing at about 40 ℃ in the final evaporation stage.

3.3. The effect of surface roughness on the nanofluid droplet sedimentary pattern

The previous sections analysed the effects of roughness on the surface wettability and silica nanofluid droplet interfacial heat and mass transfer processes during the evaporation process. In this section, we will discuss the sedimentary pattern of silica nanofluid droplets after the evaporation process and analyse its relationship with surface roughness. In this experimental study, nanofluid droplets produced a coffee-ring effect after evaporating on surfaces with different degrees of copper roughness. The sedimentary pattern of 2 μL silica nanofluid droplets on the surfaces S1 to S4 is shown in Fig. 7(a-d). As the surface roughness decreases, the sedimentary pattern becomes more precise and complete. It may be owed that as the surface roughness decreases, the substrate surface wettability decreases, and the evaporative cooling effect of the droplets is also enhanced. In this way, the temperature difference between the top and edge regions of the sessile droplet becomes more significant, which enhances the Marangoni effect inside the silica nanofluid droplet, which in turn leads to a faster and more massive aggregation of silica nanoparticles inside the droplet to the contact line region via Marangoni flow. It can be concluded that increasing the roughness of the copper surface can inhibit the coffee-ring effect to a certain extent. At the same time, it can also be seen from Fig. 7(a-d) that as the roughness increases, the coffee-ring sedimentary pattern becomes unclear, and its shape also becomes more irregular. This is because during the wetting process, after the droplet adheres to the surface, the

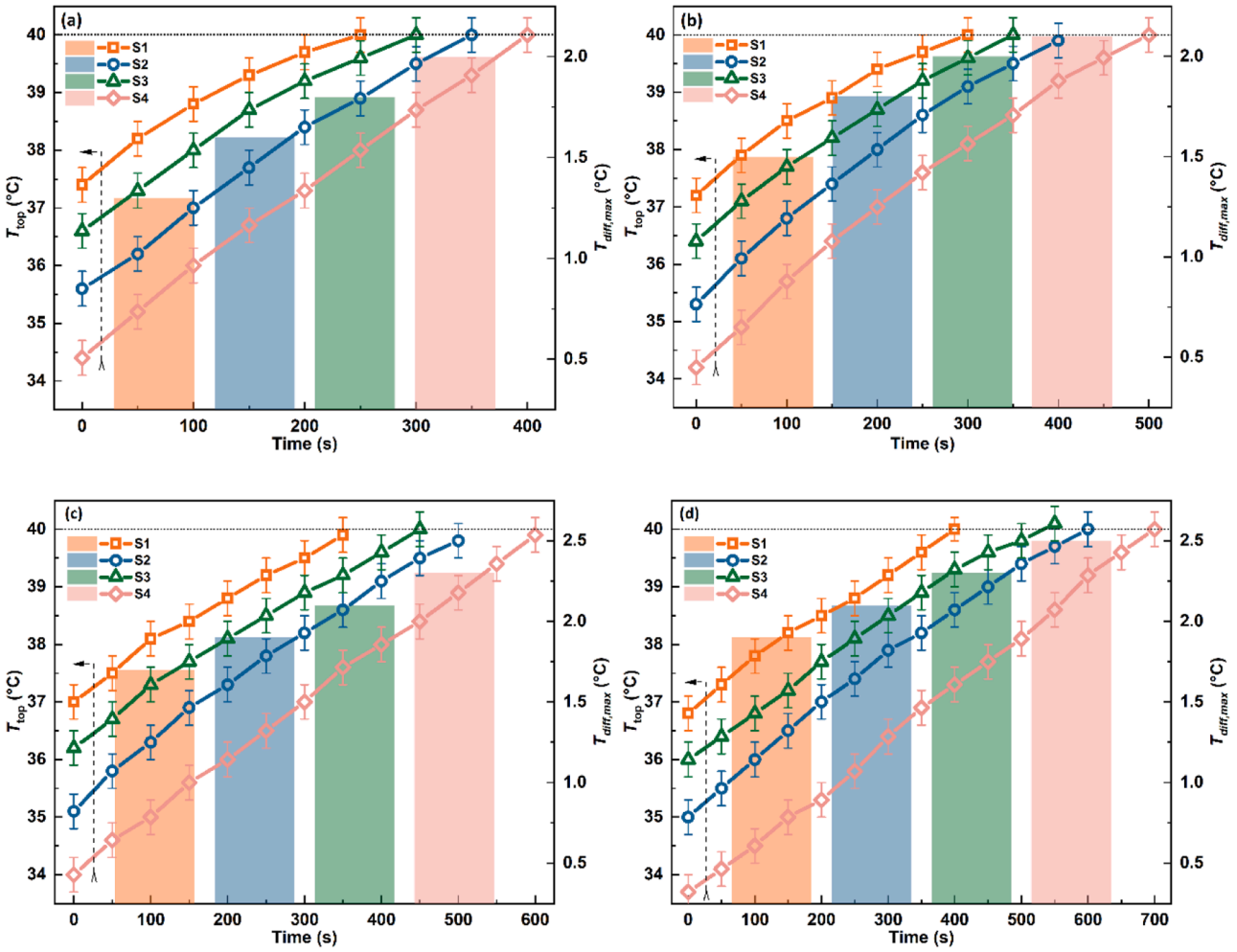

Fig. 5. The temperature change of the droplet top region T_{top} with time and the maximum temperature difference in liquid-vapour interface $T_{diff,max}$ when the droplet volume is (a) 2 μL; (b) 4 μL; (c) 6 μL; (d) 8 μL.

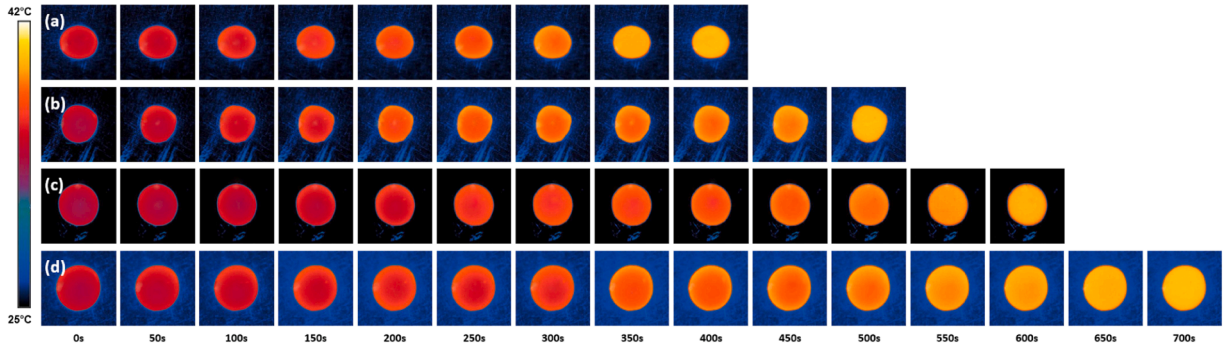

Fig. 6. The evolution of interface temperature distribution of (a) 2 μL; (b) 4 μL; (c) 6 μL; (d) 8 μL droplet on the S4 surface with time.

contact line is restricted by the large grooves on the rough surface and cannot move evenly around but is hindered, limiting the contact line's roundness and further affecting the sedimentary pattern.

At the same time, the relative height distribution statistics of the coffee-ring sedimentary pattern of silica nanofluid droplets under different roughness surfaces are shown in Fig. 8(a-d). As shown in Fig. 8 (a), the range of horizontal coordinates represents the width of the sedimentary coffee-ring pattern marked by the white line in the illustration within Fig. 8(a). h/h_{avg} represents the dimensionless height of the sedimentary coffee-ring pattern, which means the ratio of the height of each location to the overall average height. In the dimensionless height distribution of the coffee ring formed on the surface of S1, the maximum value differs from the minimum value by a factor of about 2.6. Meanwhile, as shown in Fig. 8(b-d), the difference between the maximum and minimum values of the dimensionless heights of the silica nanofluid droplets increased to about 2.7, 5.9, and 8.5 times when the droplets were located on the S2, S3, and S4 surfaces, respectively. This phenomenon is due to several reasons. Firstly, as the surface roughness degree increases, the coffee-ring phenomenon of the silica nanofluid droplet is suppressed. This makes the coffee-ring sedimentary pattern

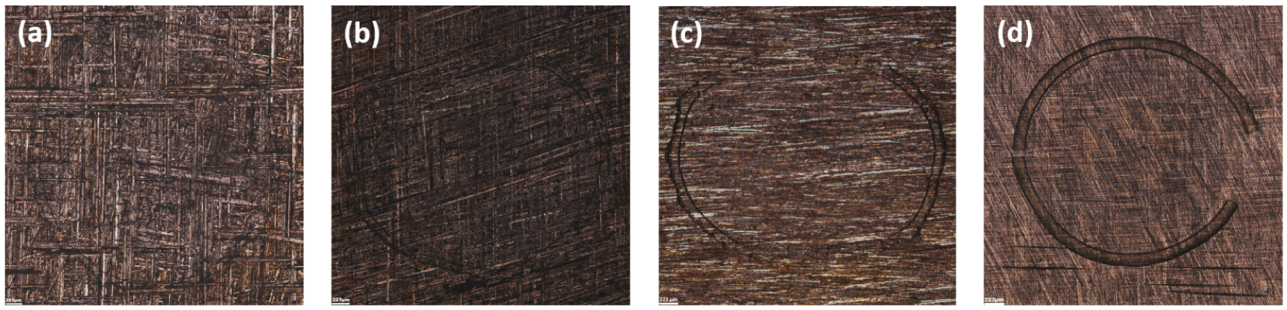

Fig. 7. The sedimentary pattern after the evaporation of 2 μL silica nanofluid droplet on the (a) S1, (b) S2, (c)S3, and (d)S4 surfaces, respectively.

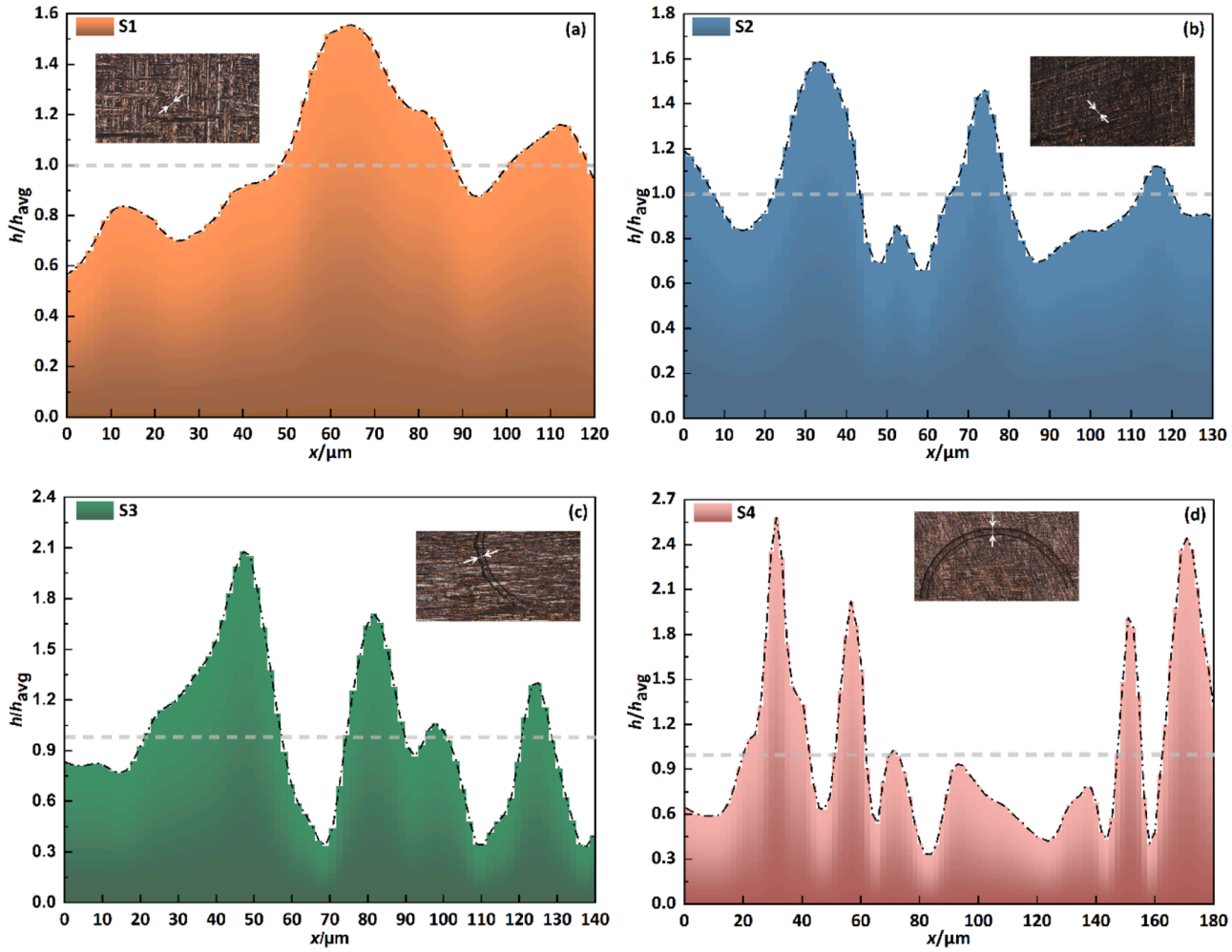

Fig. 8. Dimensionless height of the cross-section of the sedimentary ring after evaporation of a 2 μL silica nanofluid droplet on the (a) S1, (b) S2, (c) S3, (d) S4 surface.

relatively insignificant, leading to a flatter distribution of dimensionless heights. Second, as the roughness decreases, the copper substrate surface becomes smoother, allowing the silica nanoparticles to be deposited chiefly on the surface rather than in the grooves, contributing to a more differentiated distribution of dimensionless heights.

Also, the pattern of sedimentary coffee rings formed on the surface of the copper substrate after the evaporation of different volumes of silica nanofluid droplets is shown in Fig. 9, where only the roughest S1 surface and the smoothest S4 surface were selected for comparison to clarify the differences. As shown in Fig. 9(a-c), the diameter of the sedimentary coffee-ring pattern increases as the droplet volume improves. At the same time, the sedimentary coffee-ring patterns remain visible as the droplet volume increases, and all these have about 1–4 fractures. As shown in Fig. 9(c), a localized 3D surface measurement of the fractures by optical profilometer shows that there are almost no residual silica nanoparticles left at the fracture regions, which indicates that the fractures appeared abruptly after the silica nanofluid droplet evaporation and the formation of the sedimentary coffee-ring patterns. Meanwhile, it can be seen in Fig. 9(d-f) that the coffee-ring effect appears regardless of the increase in droplet volume. Still, the sedimentary coffee-ring pattern produced by the droplet's evaporation is not apparent, and the ring deposition pattern has many fractures (>10). Although the sedimentary coffee-ring patterns fractured on both surfaces, the causes differed. On the smooth surface (S4), the sedimentary coffee-ring pattern formed

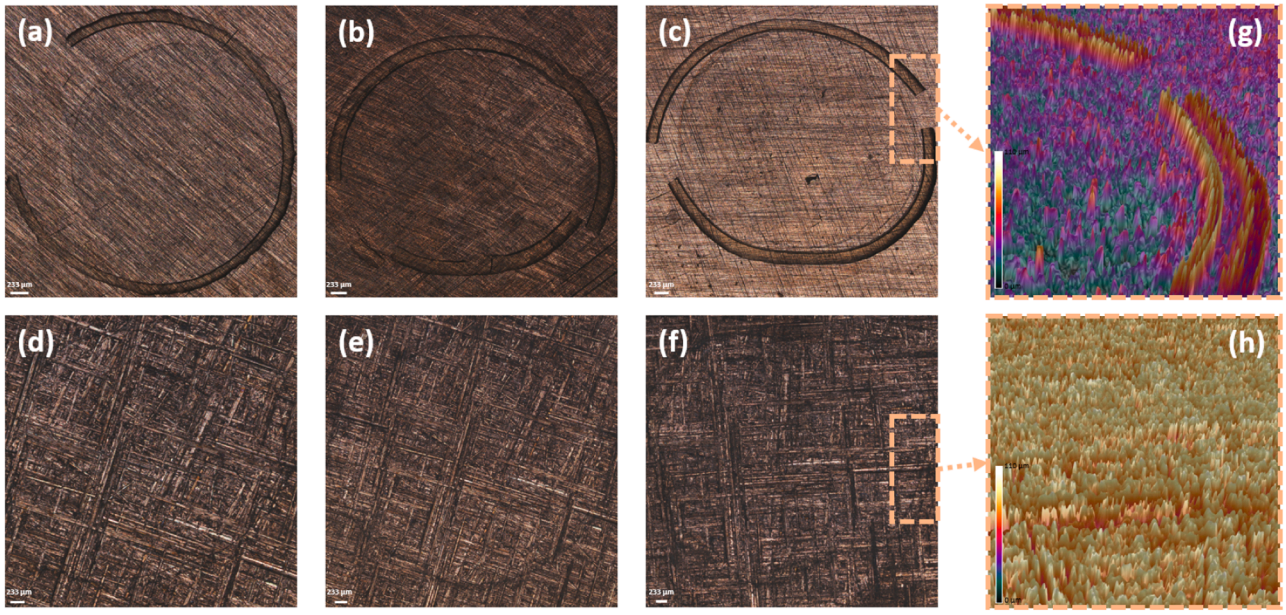

Fig. 9. Microscope images of the sedimentary coffee-ring patterns of (a) 4; (b) 6; and (c) 8 μL silica nanofluid droplets placed on the S4 surface; Microscope images of the sedimentary coffee-ring patterns of (d) 4; (e) 6; and (f) 8 μL silica nanofluid droplets placed on the S1 surface; (g) and (h) is the optical profile of the selected area.

gradually and entirely during evaporation. In contrast, the fracture may be attributed to the bottom heating, which caused the sedimentary coffee-ring pattern to receive thermal stresses. Some localized thermal stresses were stronger than the inherent strength of the silica sedimentary ring itself, and thus, a sudden fracture occurred after the evaporation was completed. Meanwhile, on the rough surface (S1), the surface grooves were much more numerous than those on the smooth surface and had a greater depth, resulting in a poorer flatness. In this way, when the nanoparticles gather and deposit toward the contact line area during the evaporation process, the coffee-ring sedimentary pattern formed by them is subject to natural uneven stress distribution at the bottom, which makes many fractures generated, so it may not be possible to form a complete and continuous ring sedimentary pattern during the evaporation process.

4. Conclusions

In this paper, the effect of copper surface roughness on the evaporation dynamics of the sessile silica nanofluids droplet is investigated experimentally. There are many studies on the evaporation phenomenon and deposition pattern of silica nanofluid droplets [34,50,51], including its deposition mechanism or the effect of surfactant addition. However, this paper is unique in that it studies the effect of surface roughness on the coffee deposition cracks of silica nanofluid droplets. The results show that based on the hydrophilic copper surface, the surface wettability increases with increasing roughness, reducing the contact angle of the nanofluid droplets. Correspondingly, the height change of droplets is not significantly affected by roughness, and the change rate is slow in the early evaporation stage and increases sharply in the later stage. Meanwhile, the evaporation of nanofluid droplets on the S1, S2, and S3 surfaces follows the CCR pattern regardless of the droplet volume. However, on the S4 surface, the evaporation is in the CCR mode in the beginning and middle stages but changes to the mixed mode in the last 10 %−20 % of the total process approximately. In addition to wettability, the experiment also observed the effect of roughness on the heat transfer process at the liquid-vapour interface of silica nanofluid droplets. As the surface roughness decreases, the adhesion work between the droplet and the solid-liquid interface also decreases. When the surface changes from S1 to S4, the initial adhesion work, on average, decreases by about 45 %. At the same time, as the roughness decreases, the temperature at the apex of the liquid-vapour interface also decreases, and the temperature difference between the top liquid-vapour interface and contact line region also increases, up to about 2.5℃, indicating that increasing the surface roughness can suppress the evaporative cooling effect of the nanofluid droplet during evaporation. Similarly, substrate roughness also impacts the coffee-ring effect of silica nanofluid droplets. As the roughness increases, the coffee-ring sedimentary pattern of the nanofluid droplets becomes less pronounced due to the dual reasons of deep surface grooves for greater roughness and suppression of the Marangoni flow. Experimental results show that forming rounded droplet and coffee ring deposition patterns on rough surfaces is challenging but accessible on smooth surfaces. On the smoother surface, there are fewer fractures in the coffee-ring sedimentary pattern, and the relative height difference of the sedimentary pattern is more pronounced, with a maximum amplitude of up to 8.5 times. Besides, regardless of the change in droplet volume, the effect of surface roughness on the sedimentary pattern remains unchanged. In inkjet printing, paint coating, plant fertilization, and even medical testing, regulating the shape and cracks of the coffee ring deposition pattern will significantly affect its effect. This study hopes to guide the research related to the effect of roughness on the evaporation of nanofluid droplets and its subsequent practical application.

CRediT authorship contribution statement

Zhihao Zhang: Writing – review & editing, Writing – original draft, Visualization, Validation, Methodology, Investigation, Formal analysis, Conceptualization. **Yuying Yan:** Writing – review & editing, Supervision, Project administration, Methodology, Investigation, Funding acquisition, Conceptualization.

Declaration of competing interest

The authors declare that they have no known competing financial interests or personal relationships that could have appeared to influence the work reported in this paper.

Data availability

No data was used for the research described in the article.

Acknowledgements

This work was supported by H2020-MSCA-RISE-778104–ThermaSMART, Royal Society (IEC\NSFC\211210) and doctoral degree scholarship of China Scholarship Council (CSC).

References

[1] J.C. Maxwell, Collected Scientific Papers, Vol. 2, CUP, 1890.
[2] C. Park, J. Seol, A. Aldalbahi, M. Rahaman, A.L. Yarin, S.S. Yoon, Drop impact phenomena and spray cooling on hot nanotextured surfaces of various architectures and dynamic wettability, Physics of Fluids 35 (2) (2023) 027126.
[3] R. Fu, Y. Yan, C. Roberts, Z. Liu, Y. Chen, The role of dipole interactions in hyperthermia heating colloidal clusters of densely-packed superparamagnetic nanoparticles, Sci. Rep. 8 (1) (2018) 4704.
[4] D. Lohse, Fundamental fluid dynamics challenges in inkjet printing, Annu Rev. Fluid. Mech. 54 (2022) 349–382.
[5] X. Li, M. Li, J. Xu, J. You, Z. Yang, C. Li, Evaporation-induced sintering of liquid metal droplets with biological nanofibrils for flexible conductivity and responsive actuation, Nat. Commun. 10 (1) (2019) 3514.
[6] J. Dieplinger, J.T. Pinto, M. Dekner, G. Brachtl, A. Paudel, Impact of Different Saccharides on the In-Process Stability of a Protein Drug During Evaporative Drying: from Sessile Droplet Drying to Lab-Scale Spray Drying, Pharm. Res. 40 (5) (2023) 1283–1298.
[7] Y. Chen, L. Guo, N. Cai, W. Sun, Y. Yan, D. Li, H. Wang, R. Xuan, Evaporation Characteristics and Morphological Evolutions of Fuel Droplets After Hitting Different Wettability Surfaces, J. Bionic. Eng. 20 (2) (2023) 734–747.
[8] B. He, A.A. Darhuber, Evaporation of water droplets on photoresist surfaces–An experimental study of contact line pinning and evaporation residues, Colloids Surf. A Physicochem. Eng. Asp. 583 (2019) 123912.
[9] Z. Wang, D. Orejon, Y. Takata, K. Sefiane, Wetting and evaporation of multicomponent droplets, Phys. Rep. 960 (2022) 1–37.
[10] P. Gurrala, S. Balusamy, S. Banerjee, K.C. Sahu, A review on the evaporation dynamics of sessile drops of binary mixtures: challenges and opportunities, Fluid Dyn. Mater. Process 17 (2) (2021) 253–284.
[11] Y.T. Aksoy, Y. Zhu, P. Eneren, E. Koos, M.R. Vetrano, The impact of nanofluids on droplet/spray cooling of a heated surface: a critical review, Energies. (Basel) 14 (1) (2020) 80.
[12] X. Zhong, A. Crivoi, F. Duan, Sessile nanofluid droplet drying, Adv. Colloid. Interface Sci. 217 (2015) 13–30.
[13] R.G. Larson, Twenty years of drying droplets, Nature 550 (7677) (2017) 466–467.
[14] R.D. Deegan, O. Bakajin, T.F. Dupont, G. Huber, S.R. Nagel, T.A. Witten, Capillary flow as the cause of ring stains from dried liquid drops, Nature 389 (6653) (1997) 827–829.
[15] G. Gold, K. Helmreich, A physical surface roughness model and its applications, IEEe Trans. Microw. Theory. Tech. 65 (10) (2017) 3720–3732.
[16] S. Croll, Surface roughness profile and its effect on coating adhesion and corrosion protection: a review, Prog. Org. Coat. 148 (2020) 105847.
[17] W.-L. Cheng, W.-W. Zhang, H. Chen, L. Hu, Spray cooling and flash evaporation cooling: the current development and application, Renew. Sustain. Energy Rev. 55 (2016) 614–628.
[18] X. Zhang, C. Yang, T. Xi, J. Zhao, K. Yang, Surface Roughness of Cu-Bearing Stainless Steel Affects Its Contact-Killing Efficiency by Mediating the Interfacial Interaction with Bacteria, ACS. Appl. Mater. Interfaces. 13 (2) (2021) 2303–2315.
[19] X. Wang, Z. Liu, L. Wang, Y. Yan, Investigation of droplet evaporation on copper substrate with different roughness, J. Bionic. Eng. 17 (4) (2020) 835–842.
[20] Y. Xiao, J. Zheng, Y. He, L. Wang, Droplet and bubble wetting behaviors: the roles of surface wettability and roughness, Colloids Surf. A Physicochem. Eng. Asp. 653 (2022) 130008.
[21] A. Askounis, K. Sefiane, V. Koutsos, M.E. Shanahan, Effect of particle geometry on triple line motion of nano-fluid drops and deposit nano-structuring, Adv. Colloid. Interface Sci. 222 (2015) 44–57.
[22] T. Furuta, T. Isobe, M. Sakai, S. Matsushita, A. Nakajima, Wetting mode transition of nanoliter scale water droplets during evaporation on superhydrophobic surfaces with random roughness structure, Appl. Surf. Sci. 258 (7) (2012) 2378–2383.
[23] S. Kumar, V. Charitatos, Influence of Surface Roughness on Droplet Evaporation and Absorption: insights into Experiments from Lubrication-Theory-Based Models, Langmuir. 38 (51) (2022) 15889–15904.
[24] T.A. Nguyen, A.V. Nguyen, M.A. Hampton, Z.P. Xu, L. Huang, V. Rudolph, Theoretical and experimental analysis of droplet evaporation on solid surfaces, Chem. Eng. Sci. 69 (1) (2012) 522–529.
[25] D. Zhang, Y. Huang, Y. Wang, Bonding performances of epoxy coatings reinforced by carbon nanotubes (CNTs) on mild steel substrate with different surface roughness, Compos. Part A Appl. Sci. Manuf. 147 (2021) 106479.
[26] A. Bussonnière, M.B. Bigdeli, D.-Y. Chueh, Q. Liu, P. Chen, P.A. Tsai, Universal wetting transition of an evaporating water droplet on hydrophobic micro-and nano-structures, Soft. Matter. 13 (5) (2017) 978–984.
[27] X. Chen, R. Ma, J. Li, C. Hao, W. Guo, B.L. Luk, S.C. Li, S. Yao, Z. Wang, Evaporation of droplets on superhydrophobic surfaces: surface roughness and small droplet size effects, Phys. Rev. Lett. 109 (11) (2012) 116101.
[28] W. Huang, X. He, C. Liu, X. Li, Y. Liu, C.P. Collier, B.R. Srijanto, J. Liu, J. Cheng, Droplet evaporation on hot micro-structured superhydrophobic surfaces: analysis of evaporation from droplet cap and base surfaces, Int. J. Heat. Mass Transf. 185 (2022) 122314.
[29] M.R. Gunjan, R. Raj, Dynamic roughness ratio-based framework for modeling mixed mode of droplet evaporation, Langmuir. 33 (28) (2017) 7191–7201.
[30] F.R. Siddiqui, C.Y. Tso, S.C. Fu, H. Qiu, C.Y. Chao, Evaporation and wetting behavior of silver-graphene hybrid nanofluid droplet on its porous residue surface for various mixing ratios, Int. J. Heat. Mass Transf. 153 (2020) 119618.
[31] F.R. Siddiqui, E.C. Tso, S.C. Fu, C.Y. Chao, H. Qiu, Experimental investigation on silver-graphene hybrid nanofluid droplet evaporation and wetting characteristics of its nanostructured droplet residue, in: Fluids Engineering Division Summer Meeting, American Society of Mechanical Engineers, 2019. V004T006A010.
[32] K. Batishcheva, G. Kuznetsov, E. Orlova, Y.N. Vympina, Evaporation of colloidal droplets from aluminum–magnesium alloy surfaces after laser-texturing and mechanical processing, Colloids Surf. A Physicochem. Eng. Asp. 628 (2021) 127301.
[33] V. Charitatos, T. Pham, S. Kumar, Droplet evaporation on inclined substrates, Phys. Rev. Fluids. 6 (8) (2021) 084001.
[34] R. Mulka, A. Kujawska, B. Zajączkowski, S. Mancin, M. Buschmann, Drying silica-nanofluid droplets, Colloids Surf. A Physicochem. Eng. Asp. 623 (2021) 126730.
[35] T. Liu, H. Luo, J. Ma, W. Xie, Y. Wang, G. Jing, Surface roughness induced cracks of the deposition film from drying colloidal suspension, European Phys. J. E 39 (2016) 1–8.
[36] P. Wąsik, A.M. Seddon, H. Wu, W.H. Briscoe, Bénard–Marangoni dendrites upon evaporation of a reactive ZnO nanofluid droplet: effect of substrate chemistry, Langmuir. 35 (17) (2019) 5830–5840.
[37] N. Kubochkin, J. Venzmer, T. Gambaryan-Roisman, Superspreading and drying of trisiloxane-laden quantum dot nanofluids on hydrophobic surfaces, Langmuir. 36 (14) (2020) 3798–3813.
[38] Y.C. Kim, Evaporation of nanofluid droplet on heated surface, Adv. Mech. Eng. 7 (4) (2015) 1687814015578358.
[39] B. Liu, Y. Liu, L. Chai, Effects of roughness and size ratio on alumina fluid deposition patterns, in: E3S Web of Conferences, EDP Sciences, 2021, p. 01016.
[40] C.J. Van Oss, Interfacial Forces in Aqueous Media, CRC press, 2006.
[41] A.A. Albert, H.S. DG, P. V, Review of stability enhanced nanofluids prepared by one-step methods—Heat transfer mechanism and thermo-physical properties, Chem. Eng. Commun. 210 (10) (2023) 1822–1852.
[42] R.K. Mudidana, V. Miditana, V. Rambabu, Synthesis of nanofluids preparation–A review, Mater. Today Proc. (2023).
[43] J. Wang, X. Yang, J.J. Klemeš, K. Tian, T. Ma, B. Sunden, A review on nanofluid stability: preparation and application, Renew. Sustain. Energy Rev. 188 (2023) 113854.
[44] M. Bhuiyan, R. Saidur, M. Amalina, R. Mostafizur, A. Islam, Effect of nanoparticles concentration and their sizes on surface tension of nanofluids, Procedia Eng. 105 (2015) 431–437.
[45] A. Kujawska, R. Mulka, S. Hamze, G. Żyła, B. Zajaczkowski, M.H. Buschmann, P. Estellé, The effect of boiling in a thermosyphon on surface tension and contact angle of silica and graphene oxide nanofluids, Colloids Surf. A Physicochem. Eng. Asp. 627 (2021) 127082.
[46] D. Brutin, Droplet Wetting and evaporation: from Pure to Complex Fluids, Academic Press, 2015.
[47] X. He, J. Cheng, C.P. Collier, B.R. Srijanto, D.P. Briggs, Evaporation of squeezed water droplets between two parallel hydrophobic/superhydrophobic surfaces, J. Colloid. Interface Sci. 576 (2020) 127–138.
[48] H. Gelderblom, C. Diddens, A. Marin, Evaporation-driven liquid flow in sessile droplets, Soft. Matter. 18 (45) (2022) 8535–8553.
[49] R. Picknett, R. Bexon, The evaporation of sessile or pendant drops in still air, J. Colloid. Interface Sci. 61 (2) (1977) 336–350.
[50] M.A. Hampton, T.A. Nguyen, A.V. Nguyen, Z.P. Xu, L. Huang, V. Rudolph, Influence of surface orientation on the organization of nanoparticles in drying nanofluid droplets, J. Colloid. Interface Sci. 377 (1) (2012) 456–462.
[51] X.-Y. Yang, G.-H. Li, X. Huang, Y.-S. Yu, Evaporative deposition of surfactant-laden nanofluid droplets over a silicon surface, Langmuir. 38 (38) (2022) 11666–11674.